Ion Density Profiles behind Shock Waves in Air

A. FROHN* AND P. C. T. DE BOER†
Cornell University, Ithaca, N. Y.

Experimental results are reported for the ionization rate behind shock waves of Mach numbers between 7.2 and 9.2. The results were obtained using a hollow, total collector probe in combination with a 38-mm-diam, stainless steel shock tube designed to minimize the impurity level in the test gas. Good agreement was obtained with a theoretical result based on Lin and Teare's rate equations. Equilibrium ion densities in good agreement with theory were measured behind shocks of Mach number 7.2–12.8, with initial pressures between 0.5 and 40-mm Hg. The effects on the measurements of deviations from ideal shock tube flow were determined to be small. Ion densities measured range from 10^8 to 10^{12} cm^{-3}. At the higher ion densities there are large space charge effects inside the probe. Under these circumstances, proper operation of the probe still could be obtained provided the collector potential was not made too high. This implies that the mobility of the NO ions collected must be rather large.

I. Introduction

ION density profiles behind shock waves in air have been the subject of various recent investigations. Lin, Neal, and Fyfe[1] made measurements in a low-density shock tube using microwave techniques and a magnetic induction device, in the range of shock Mach numbers M_s between 14 and 20. A theoretical analysis of their results based on chemical rate equations was given by Lin and Teare.[2] Experimental results for even higher shock Mach numbers were reported by Wilson,[3] who found that for shock Mach numbers above 27, electron densities become high enough so that electron impact reactions become dominant. At the lower temperature end experimental data have been obtained by Thompson,[4] who used a low-density shock tube in combination with microwave techniques, with infrared emission measurements, and with a hollow, total collector probe described by de Boer.[5]

The present investigation was undertaken in order to extend the range of measured profiles to still lower temperatures. At these temperatures, both the ion density and the ionization relaxation rate become much smaller, and it is impractical to use a low-density shock tube because the test time required is too long. A 38-mm-diam shock tube was used in combination with the hollow, total collector probe of Ref. 5. This probe has a very high sensitivity and can be used without difficulty in the regime of interest. The main problem to be overcome was the influence of impurities on the ionization rates. This problem could be solved by using great care in the experimental procedures.

II. Experimental Details

The ion density profile behind the shock wave was measured using a hollow, total collector probe previously described in Ref. 5. The probe consists of a hollow circular glass tube with its axis parallel to the flow. Two pairs of electrodes are painted on the inside surface of the probe, as shown in Fig. 1a. A constant voltage is applied across each pair of electrodes, so that charged particles entering the probe will drift towards the electrodes. When the drift velocity is large enough, all charged particles are collected by the first pair of electrodes. The ion current to the negative electrode is given by the relation

$$j_i = n_i A U e \tag{1}$$

where A is the probe entrance area, n_i the ion density, U the gas velocity, and e the charge per particle. The second pair of electrodes should attract negligible current, and serves to provide a check on the proper operation of the probe.

The shock tube was designed from the point of view that the impurity level in the test gas should be minimized. In order to keep the outgassing from the tube walls as low as possible, the tube was made of stainless steel and the inside was honed to a 0.5-μ finish. Viton-A O-rings were used throughout the shock tube, and the entire low-pressure section could be baked at 120°C. The pumping station for the shock tube consisted mainly of a two-stage mechanical pump with a zeolite foreline trap, a four-stage stainless steel oil diffusion pump, and a continually operated 5-cm Granville-Phillips liquid nitrogen cold trap. Above this cold trap were 5-cm Ultek high-vacuum fittings made of stainless steel and equipped with copper gaskets. An all stainless steel bellows valve connected the pumping system to the shock tube. Upon closing the main valve between shock tube and pumping system, an ultimate vacuum of 2×10^{-8} mm Hg could be obtained just before this main valve. After a baking period of 5 hr, a pressure of 7×10^{-8}-mm Hg was

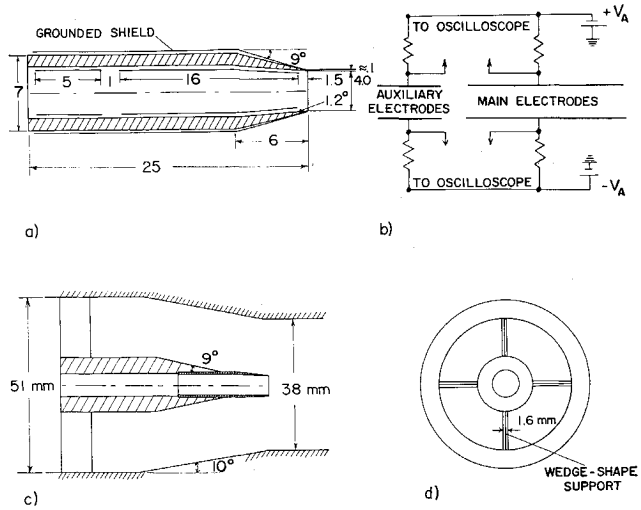

Fig. 1 Hollow, total collector probe: a) dimensions of probe (mm), b) electronic circuit, c and d) position in shock tube.

Received July 18, 1966; revision received September 26, 1966; also presented as Paper 67–94 at the AIAA 5th Aerospace Sciences Meeting, New York, January 23–26, 1967. This work was supported by the U. S. Office of Naval Research. Reproduction in whole or in part for any purpose of the United States Government is permitted. We are very grateful to W. P. Thompson[4] for making his results available to us before final publication.

* Research Associate, Graduate School of Aerospace Engineering; now Wissenschaftlicher Assistent am Lehrstuhl für Mechanik, Technische Hochschule, Aachen, Germany.

† Assistant Professor, Graduate School of Aerospace Engineering. Member AIAA.

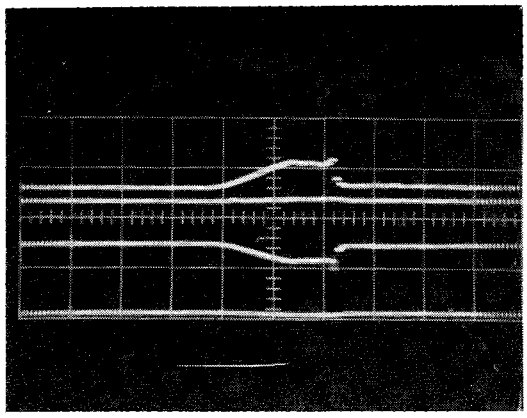

Fig. 2 Oscillogram obtained at shock Mach number M_s = 8.0 and initial pressure p_1 = 14-mm Hg. Traces, from top to bottom: main ion collector, auxiliary ion collector, main electron collector, auxiliary electron collector. Time proceeds from left to right. Horizontal scale 50 μsec/div, vertical scales all 0.2 v/div, load resistors all 180 Ω, ion collectors at −25 v, electron collectors at +3 v. Derived data: T_{equil} = 3000°K, $(\rho_2/\rho_1)_{equil}$ = 7.6, $U_{equil} = 2.4 \times 10^5$ cm/sec, n_i (equil) = 1.1×10^{11} cm^{-3}, τ = 60 sec, and t_ρ = 5 μsec.

obtained inside the shock tube. Upon ceasing to pump by closing a secondary valve, located right above the cold trap, the pressure in the shock tube was found to increase over the value just given at the rate of 0.1-μ Hg/h. The length of the low-pressure section was 6.20 m. The probe was located 1 m ahead of the end of this section, so that no reflected waves could reach the test section during the measurements. In order to avoid choking of the flow around the probe and the probe holder, the inside diameter of the shock tube increased from 38 to 51 mm at the location of the probe, as shown in Fig. 1c. The entrance area of the probe was located just inside the 38-mm section. The probe is slightly tapered on the inside to compensate for the displacement effect of the boundary layer. The probe has a sharp leading edge so that a standing bow shock ahead of the probe can be avoided. An analysis of various requirements that must be fulfilled in order to obtain a satisfactory flow pattern about the probe was given in Ref. 5. This analysis was followed in designing the present probe.

The shock wave speed was measured with thin film heat-transfer gages, which consisted of platinum paint strips backed by pyrex. The pyrex was made out of 7-mm-thick rods, the end surfaces of which were ground flush with the inside wall of the shock tube. The rods were mounted with Varian Torr Seal in stainless steel plugs, which were sealed with Viton-A O-rings to the shock tube. These gages were located 7.6, 24.0, and 158 cm, respectively, ahead of the probe. The average shock speed between the last two stations was somewhat smaller than that between the first two, but the difference was never more than 5%. Once this was established, the first gage usually was used only to obtain a trigger signal for the oscilloscopes, while the measurement of the shock speed was obtained from the other two gages. The bias voltages for the electrodes of the collector probe were provided by dry batteries. The electrode current was measured as a voltage drop across a load resistor of 0.18, 3.3, or 15 kΩ which, in connection with a cable capacity of 200 pF, resulted in response times of 0.04, 0.7, and 3 μsec, respectively.

The experiments were carried out using commercial dry air with a specified hydrocarbon content of less than 2 ppm supplied by the Matheson Company. During a few minutes before each run, the test gas was passed through the shock tube via a liquid nitrogen cold trap. The gas pressure inside this trap was about equal to the pressure in the test section, which was 40-mm Hg at most. This precluded the possibility of oxygen condensation inside the cold trap, since the vapor pressure of oxygen is about 150-mm Hg at the boiling temperature of liquid nitrogen at atmospheric pressure.[6] The tubing between cold trap and shock tube was long enough to obtain restoration of the gas temperature to essentially room temperature. At the other end of the shock tube the gas was continually removed by a mechanical pump, after first having passed through another liquid nitrogen cold trap, a large dump tank, and a zeolite foreline trap. Thus the impurity level arising from outgassing of the shock tube could be reduced to 5 parts in 10^9 for an initial pressure of 10-mm Hg. The pressure in the test section was measured on an NRC-Alphatron vacuum gage type 520 B. After the pressure reached its steady-state value, the valve to this gage was closed and the diaphragm was broken by increasing the pressure in the driver section. Either helium or hydrogen could be used as the driver gas. The diaphragm consisted of aluminum sheet of 1-mm thickness, scribed to an approximate depth of 0.4 mm by using a scriber instrument provided with a glass cutter.

III. Experimental Results

Experimental data have been obtained for shock Mach numbers between 7.2 and 12.8 with initial pressures between 0.5- and 40-mm Hg. A representative oscillogram of the ion and electron collector currents is shown in Fig. 2. The currents collected by the first (main) electrodes are displayed, as well as those collected by the second (auxiliary) electrodes. The latter are quite small compared with the former, implying that Eq. (1) may be used to obtain the charged particle density from the main signal. The main ion signal was found to be independent of the ion collector voltage over the range of 20–90 v. On the other hand, the main electron signal was dependent on the electron collector voltage. This dependence was also reported in Ref. 5, and is believed to arise from the large mobility of the electrons. Because of this large mobility, even a small axial component of the electric field at the probe entrance will influence the number of electrons entering the probe. Figure 2 is the result of one experiment out of a series in which the voltage on the electron collectors was varied from +2 to +8 v. This resulted in variations of the amplitude of the electron signal from 1 to 6 times that of the ion signal, respectively. The ion signal again was found not to vary in these experiments. In view of this, only the ion currents were used to obtain data on the ionization profiles behind the shock.

The main signal in Fig. 2 begins to rise after the arrival of the shock front and eventually reaches an approximately con-

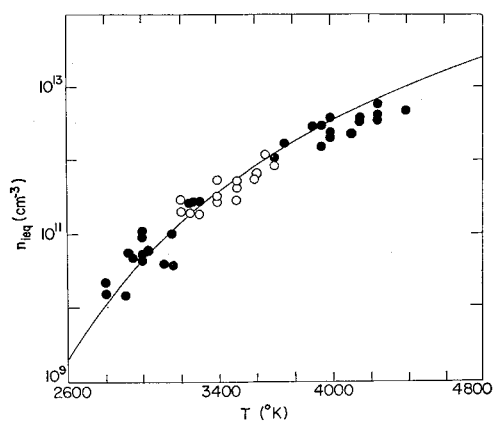

Fig. 3 Equilibrium ion density n_i (equil) as a function of equilibrium temperature T_{equil}. Open points are results obtained at an initial pressure of 4-mm Hg; closed points are results obtained at different initial pressures p_1, reduced to equivalent values at 4-mm Hg by multiplication with $[4/p_1(\text{in mm Hg})]^{1/2}$. Line is theoretical result based on the tables of Refs. 7 and 8.

stant value. A characteristic relaxation time τ for the ionization process is obtained from these oscillograms by using the relation

$$\tau = n_i(\text{equil})/(dn_i/dt)_{\max}$$

where $(dn_i/dt)_{\max}$ is the maximum ion density gradient, and n_i(equil) is the equilibrium value of the ion density as measured from the oscillogram. Although there may be an "induction time" between arrival of the shock wave and start of the rise of the signal, no meaningful measurement of such a time has been made.

The equilibrium ion densities measured are shown in Fig. 3 as a function of equilibrium temperature. All data were reduced to equivalent values at a reference pressure $P_1 = 4$-mm Hg by multiplying the value of n_i(equil) measured with the square root of the reference pressure over the actua initial pressure. Also shown is a theoretical result obtained using the graphs and tables of Refs. 7 and 8. The experimental points in general are rather close to the theoretical curve. The main origin of the scatter is believed to be the uncertainty in the measurement of the shock velocity, which arose from the use of a cathode-ray beam chopped at a frequency of 2 Mc/sec. For equilibrium temperatures below approximately 3400°K, the records obtained all had the character of Fig. 2. In order to attain equilibrium temperatures above 3400°K, rather strong shocks are required, which could be generated only at small initial pressures P_1. Under these circumstances, the effects of boundary layers on the flow behind the shock wave may become quite pronounced. As a result, the temperature and the density behind the shock both increase, and therefore the equilibrium ion density also increases. Examples of this behavior are shown in Fig. 4. The maximum increase of n_i(equil) which may be encountered corresponds to stagnation conditions of the flow behind the shock. These would occur at the contact surface, if this surface moves at the same speed as the shock front, and if cooling of the test gas near the contact surface is negligible.

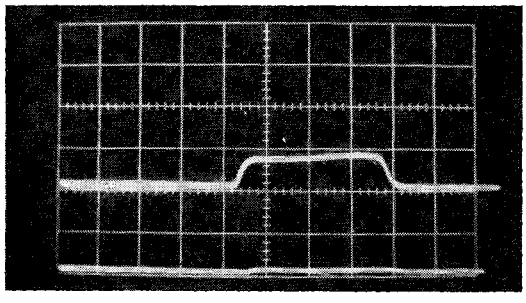

a) Oscillograms obtained at $M_s = 10.3$, $p_1 = 4$-mm Hg

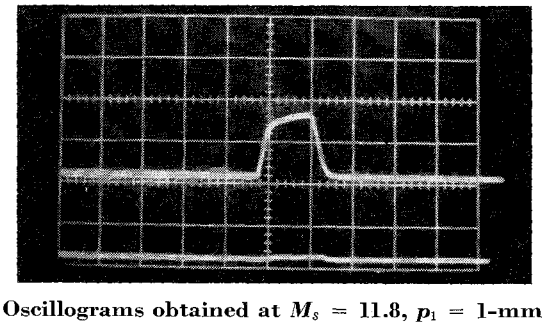

b) Oscillograms obtained at $M_s = 11.8$, $p_1 = 1$-mm Hg

Fig. 4 Oscillograms obtained. Upper traces are derived from main ion collector, lower traces from auxiliary ion collector. Vertical scale, all traces, 20 v/div. Load resistors 3.3 kΩ, ion collectors at −30 v, electron collectors at 0 v. Horizontal scale a) 20μ sec/div, b) 50μ sec/div. Derived data: a) $T_{\text{equil}} = 3550$°K, $(\rho_2/\rho_1)_{\text{equil}} = 10.0$, $U_{\text{equil}} = 3.2 \times 10^5$ cm/sec, n_i (equil = 6.3) $\times 10^{11}$ cm^{-3} b) $T_{\text{equil}} = 4150$°K, $(\rho_2/\rho_1)_{\text{equil}} = 10.7$, $U_{\text{equil}} = 3.7 \times 10^5$ cm/sec, n_i (equil) $= 1.1 \times 10^{12}$ cm^{-3}.

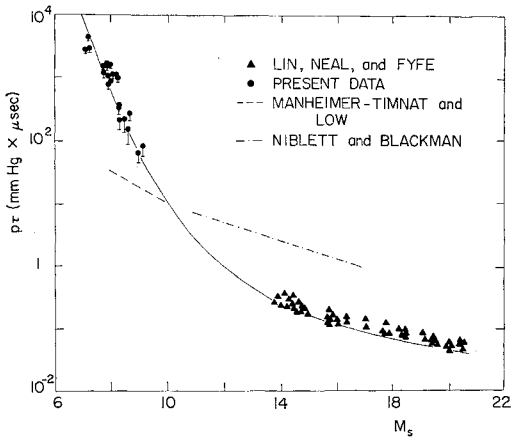

Fig. 5 Product of relaxation time τ and initial pressure p_1 as function of shock Mach number M_s. Solid line is theoretical result of Lin and Teare.[2,4] Present data are given by dots (τ), and by horizontal bars (τ minus probe transit time t_p).

This maximum increase of n_i(equil) was calculated with the aid of Refs. 7 and 8, and was found to be of order 10% for the conditions of interest, which is in approximate agreement with the experimental records obtained at these higher temperatures.

It is interesting to note that the ion densities measured range from 10^8 to 10^{12} cm^{-3}. This range includes results obtained in the nonequilibrium regions. Previous measurements, using the hollow, total collector probe, were successful only in the range below 10^{10} cm^{-3}; proper operation at higher densities presumably was prevented by space charge effects. The present results at $n_i > 10^{10}$ cm^{-3} were obtained with the relatively low collector voltage of 30 v; increasing this voltage beyond 90v resulted in sizeable currents on both electrodes, or even in electric breakdown. Apparently, secondary ionization can occur easily under these conditions, but as long as it is avoided the probe will operate properly in spite of the space charge effects that must occur. The smallness of the collector voltage implies that the ion mobility k must be rather high. As a crude estimate we obtain $k = 2 \times 10^4$ cm^2 v^{-1} sec^{-1} for a density 10^{-3} times the density at N.P.T., compared to 2.5×10^3 cm^2 v^{-1} sec^{-1}, which is the result of an estimate given in Ref. 5. Presumably, this high mobility arises because the ions are newly created, and no clusters have formed around them. This would be analogous to the high mobility of newly formed negative ions described by Cobine,[9] who notes that this occurs only when very few impurities are present in the gas.

The results for the relaxation time τ are plotted in Fig. 5, which gives $P_1\tau$ as a function of shock Mach number M_s. Also shown are the data points obtained by Lin, Neal, and Fyfe,[1] and the approximate location of the results of Niblett and Blackman,[10] and Manheimer-Timnat and Low.[11] The latter two sets of data are based on indirect measurements of the ionization profile, namely, measurements of the luminosity; and as indicated by Lin et al.,[1] there is some doubt about their accuracy.‡ Figure 5 furthermore shows a theoretical result based on Lin and Teare's rate equations.[2] For $M_s < 14$, this result was evaluated by Thompson,[4] who used a three times larger value for the rate constant K of the reaction $N + O \rightarrow NO^+ + e$ than the value assigned to by the former authors. This change, which in fact was first suggested by Lin and Teare[2] (see below), was required in order to fit the result for τ to Thompson's experimental data. Thompson also varied several of the other rate constants pertinent to the ionization process, but this had little effect on τ. The

‡ In addition to the references cited, direct measurements of τ using microwave techniques have been carried out in Russia. For a preliminary account of this work, see Ref. 13.

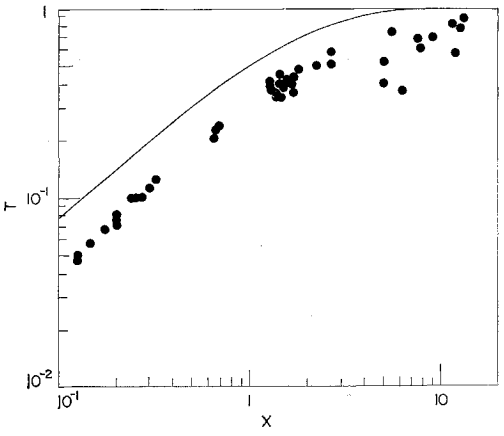

Fig. 6 Dimensionless test time T as a function of dimensionless distance X. Line is theoretical result given by Eq. (2).

agreement between the theoretical result and the present data is seen to be good. For $M_s > 14$ the theoretical result shown in Fig. 5 is one calculated by Lin and Teare,[2] using also the three times larger value for K. Although this upward revision gave improved agreement with the experimental points of Ref. 1, near-perfect agreement could be obtained by using a factor of 2 instead of 3. Lin and Teare were of the opinion, however, that such fine adjustments might not be justified at the time they wrote their paper, in view of uncertainties in their theoretical model. It now appears that this model should best be used in combination with the upward revision of the rate constant K.

In evaluating τ, we were faced with the difficulty that for many experiments the value obtained was close to the characteristic probe transit time t_p, given by the electrode length divided by the shock velocity. Only results in which $\tau/t_p > 2$ were included in Fig. 5. The remaining results are regarded as inaccurate as far as the measurement of τ is concerned, although they still gave upper limits for τ, and also gave correct values for n_i(equil). For each datum point plotted, the value of $t - \tau_p$ was calculated. This value may be regarded as a lower limit for the relaxation time, and therefore is included in Fig. 5.

It may be mentioned that oscillograms such as Figs. 2 and 4 could be obtained only when the impurity level was sufficiently low. The permissible impurity level decreases when the temperature behind the shock becomes smaller. If the impurity level is too high, the relaxation times obtained are much shorter than those given in Fig. 5. The corresponding records usually show an overshoot in ion density closely behind the shock. After the shock tube has been thoroughly cleaned at least once by pumping and baking, the results become highly reproducible. Typically, for given driver pressure and test gas pressure, oscillograms are reproduced within 10%.

In order to establish that the decrease of the signal is related to the arrival of the contact surface, the time τ_t from the beginning of the signal to the beginning of the decrease has been compared with Mirels' theoretical results[12] for the test time in low-pressure shock tubes. The dimensionless test time $T = \tau_t M_s a_1/l_m$ has been plotted in Fig. 6 against the dimensionless distance $X = (T + x/l_m)\rho_1/\rho_2$. Here a_1 is the velocity of sound ahead of the shock, l_m the asymptotic length of the test gas column as given by Fig. 6 of Ref. 12, X is the distance between the diaphragm and the test station, and ρ_2/ρ_1 is the density ratio across the shock. According to Ref. 12, the relation between X and T is given with sufficient accuracy by

$$X = 2[-\ln(1 - T^{1/2}) - T^{1/2}] \tag{2}$$

which relation is also plotted in Fig. 6. Although the agreement between theory and experiment is not very good, it is close enough to make acceptable the interpretation of the decrease as the arrival of the contact surface.

We conclude from the present results that the hollow, total collector probe of Ref. 5 can be used over a wide range of ion densities. For the experiments reported, this range covers about four orders of magnitude. For ion densities of 10^8 cm^{-3} the currents collected are still of the order of 1 μa and much lower particle densities can in principle be measured. In the present work we were limited in this respect because below $T_{\text{equil}} = 2800°$K the relaxation time became larger than the test time, but for different experimental conditions the large sensitivity of the probe may be very attractive.

References

[1] Lin, S. C., Neal, R. A., and Fyfe, W. I., "Rate of ionization behind shock waves in air. I. Experimental results," Phys. Fluids **5**, 1633–1648 (1962).

[2] Lin, S. C. and Teare, J. D., "Rate of ionization behind shock waves in air. II. Theoretical interpretations," Phys. Fluids **6**, 355–375 (1963).

[3] Wilson, J., "Ionization rate of air behind high speed shock waves," Avco Research Rept. 222 (1965).

[4] Thompson, W. P., "Ionization and NO production in air at 3000°–5000°K," Bull. Am. Phys. Soc. **10**, 727 (1965); also private communication (1966).

[5] de Boer, P. C. T., "Probe for measuring ion density in slightly ionized, high speed flow," Rev. Sci. Instr. **37**, 775–785 (1966).

[6] Hornig, R. E. and Hook, H. O., "Vapor pressures of common gases," RCA Rev. **21**, 360 (1960).

[7] a) Lewis, C. H. and Burgess, E. G., "Charts of normal shock wave properties in imperfect air," Arnold Engineering Development Center, AEDC-TDR-64-43 (1964); b) Lewis, C. H. and Neal, C. A., "Specific heat and speed of sound data for imperfect air," Arnold Engineering Development Center, AEDC-TDR-64-36 (1964); and c) Lewis, C. H. and Burgess, E. G., "Charts of normal shock wave properties in imperfect air (supplement: M_s = 1 to 10.)," Arnold Engineering Development Center, AEDC-TDR-65-196 (1965).

[8] Hilsenrath, J. and Klein, M., "Tables of thermodynamic properties of air in chemical equilibrium including second virial corrections from 1500° to 15,000°K," Arnold Engineering Development Center, AEDC-TR-65-58 (1965).

[9] Cobine, J. D., *Gaseous Conductors* (Dover Publications, New York, 1958), p. 38.

[10] Niblett, B. and Blackman, V. H., "An approximate measurement of the ionization time behind shock waves in air," J. Fluid Mech. **4**, 191–194 (1958).

[11] Manheimer-Timnat, V. and Low, W., "Electron density and ionization rate in thermally ionized gases produced by medium strength shock waves," J. Fluid Mech. **6**, 449–461 (1959).

[12] Mirels, H., "Test time in low-pressure shock tubes," Phys. Fluids **6**, 1201–1214 (1963).

[13] Bazhenova, T. V. and Lobastov, Y. S., "The measurement of the time for the establishment of an equilibrium electron concentration behind a shock wave in air," Soviet Phys. Doklady **8**, 636–638 (1964).